Engineered Science
DOI: https://dx.doi.org/10.30919/es1370

# Empowerment of Photonics in Thin Film Amorphous Silicon Solar Cells

Jagannadha Naga Pavan Kumar Chintala,[1] Sundhar Arumugam,[2] Raghvendra S. Dubey,[3] Sigamani Saravanan[4,*] and Kotari Srinivasarao[5]

## Abstract

In this paper, we investigated the light trapping mechanism of thin-film amorphous silicon (a-Si) solar cells using rigorous coupled wave analysis (RCWA) method. Using optical modeling, the distributed Bragg's reflector (DBR) is optimized and consists of alternative layers of Si and $SiO_2$ materials. The optical reflectivity of distinct DBR layers was investigated by changing various center wavelengths (400, 600, 800 and 1000 nm). These reflectance spectra showed higher or wider photonic band gap shifts due to the thickness of each layer and incident wavelength. Further, the studied new conformal thin-film solar cell architecture includes nanostructures (indium tin oxide anti-reflection coating and silver nanogratings) and optimized DBR used as backreflector. The DBRs and nanogratings helped to fold back the shorter and longer wavelength of light towards the active (a-Si) region and enhanced photon path length and life time of photon. Under normal radiation, the collection of the photons was enhanced, and also the charge carriers (electron-hole) pair generations were remarkably improved in active regions with low recombination losses. These nanostructures yielded a better light harvesting mechanism and the highest current density of 25.16 mA/cm$^2$.

*Keywords:* Light trapping; silicon; Photonic band gap; Distributed Bragg's Reflector; Back reflector.
Received: 05 May 2024; Revised: 05 November 2024; Accepted: 15 November 2024.
Article type: Research article.

## 1. Introduction

The thin film solar cell is promising and leading in to the photovoltaic (PV) market. Generally, the silicon-based materials are playing crucial role by garnering great attention due to their highest conversion cell efficiency with low-cost fabrication. Majorly, it depends on the crystalline silicon (c-Si), amorphous silicon (a-Si), polycrystalline silicon (psi), and micro-crystalline (μ-Si) silicon due to the natural abundance and is well suited to advanced technology.[1-3] Thin film technology has disadvantages, such as the lowest cell efficiency in the longer (infrared) spectral regions due to poor absorption of the photons. This issue could be solved by novel metallic or dielectric nanostructures. It might be responsible for the better light trapping scheme (textured) which needs to be controlled. In the PV module, one-dimensional (1D) photonic crystals, two-dimensional (2D) photonic crystals, and three-dimensional (3D) photonic crystals play pivotal roles in the enhancement of the light-harvesting mechanism. Lee et al. and Fink *et al.* found 1D photonic crystals fulfilled the required omnidirectional reflector rather than 2D-and 3D photonic crystals.[4,5] Recently, 1D photonic crystal has received a notable optical performance in thin film solar cells. To improve the light-harvesting mechanism (or) the collection of the photons, various nanostructures are used, such as antireflection coatings (ARC), 1D photonic crystals (1DPCs), metallic (or dielectric) nanorods, nano gratings, nanoparticles have been proposed by distinct researchers.[6-10] Among these nanostructures, 1DPC/DBR(distributed Bragg reflector), dielectric, and metallic nano gratings had shown promising absorption. Presently, the multiple nano gratings are playing an important role in solar cells and garnering great attention from various researchers.[11] Anna Starczewska and Miroslawa

[1] *Department of Engineering Physics, S.R.K.R. Engineering College (A), Bhimavaram (AP), 534204, India*
[2] *Department of ECE, PKIET, Karaikal, Puducherry, 609603, India*
[3] *Department of CS&AI, SR University, Warangal, Telangana, 536371, India*
[4] *Department of Science & Humanities, Swarnandhra College of Engineering & Technology (A), Narsapur, West Godavari (AP), 534280, India*
[5] *Department of Applied Sciences and Humanities, Sasi Institute of Technology and Engineering, Tadepalligudem, Andhra Pradesh, 534101, India*
**Email:* shasa86@gmail.com (S. Saravanan)

Kepinska (2024) explored the significance of different photonic crystals (1D, 2D & 3D). They investigated the recent developments and trends in designing photonic crystals for PV applications.[12] Karthika Sankar *et al*. (2022) presented the effect of 1D PCs using MATLAB for solar cell applications. They theoretically demonstrated and optimized the impact of ARC and distributed Bragg's reflector (DBR). Finally, the triple layer of ARC and single DBR layer boosted the cell efficiency of solar cells.[13] Rahul Kumar Ganwar *et al*. (2023) stated that the photonic crystals have excellent light field confinement and no. of various incident angles that control the light trapping mechanism in solar cells.[14] Andrea Cordo (2023) demonstrated the nanopatterned back-reflector enhanced near-field/far-field scattering mechanism in Si (active layer) related multijunction (GaInP/GaInAsO//Si) solar cells. Overall, the power conversion cell efficiency significantly improved to 0.9% compared to the reference cell structure.[15] Sigamani *et al*. (2023) investigated the effect of DBR layers in thin film amorphous silicon solar cells (a-Si) by an optimization process. Using the plane wave expansion method, various parameters were optimized, and the broader photonic band gap (PBG) was observed. Because of this tuned PBG, a-Si thin film solar yielded improved light absorption.[16] Overall, these literature reviews revealed the best light harvesting observed in between ultraviolet and visible spectral regions. However, in the near and far infrared spectrum (>700 nm), less light harvesting mechanism was noticed due to the lowest conversion cell efficiency achieved. Considerably, those longer wavelengths of light trapping mechanisms could be focused on the best PV cell.

In this letter, we focused on an improvement of light trapping in thin film a-Si solar cells by integration of front ITO-nano gratings, triangular bottom (Ag) nano gratings, and different DBRs ($Si/SiO_2$). First, suitable DBR layers are employed by changing the center wavelengths (400, 600, 800, and 1000 nm) and noticing the optimized PBG. These integrating DBR layers are used as back-side reflectors in a-Si thin film solar cells. In addition, the ITO ARC layer is at the front side of the cell, and silver (Ag) triangular grating is placed at the bottom of the active (a-Si) region to enhance light harvesting. This engineering scheme is expected to improve the light photon path length and lifetime and finally generate better cell efficiency (16.5%) and current density (25.16 mA/cm2), which was not reported within the 40 nm thick a-Si active region under the transverse electric (TE) field polarization mode. Adopting metallic nano gratings and DBR reflectors is favorable to enhancing absorption.

## 2. Designing approach

In the simulation, a commercial rigorous coupled wave analysis (RCWA) method was used, which was provided by the RSoft synopsis tool. The schematic diagram of the simulation model and corresponding fields are depicted in Fig. 1.

The DBR layers consist of two alternative materials by maintaining higher refractive index contrast like silicon (Si, $n_H$=3.5) and silicon dioxide ($SiO_2$, $n_L$=1.45).[16] This silicon based material (Si, a-Si and $SiO_2$) are abundant in nature.[12] The refractive indices are defined (or calculated) as:

$$n_i = \frac{\gamma\lambda}{4\pi} \quad (1)$$

where λ is the wavelength, γ is an exponential loss coefficient.[17] The periodic multilayers and highest refractive indexed materials are useful for the broader photonic band gap reported by Zhang *et al.* They found a good agreement between the numerically simulated and experimentally fabricated structures.[18]

Consequently, the geometric thickness of the two alternative layer thicknesses calculated by quarter-wave equations,

$$d_i = \frac{\lambda c}{4n_i} \quad (2)$$

where $n_i$ is the refractive index of the materials, and $\lambda_c$ is the center wavelength of the incident light.[19] Using the quarter wave criterion (Eq. 2), the thickness of the Si and $SiO_2$ layers was calculated with respect to the incidence wavelength and the lattice constant, as tabulated in Table 1. The designing of 1D PCs are with respect to the selection of the center wavelength (λc = 400, 600, 800 and 1000 nm), refractive index (n) of the materials and a number of multilayers.

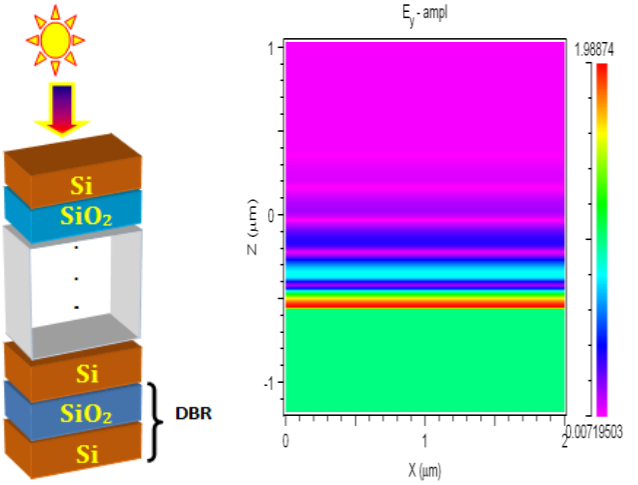


(a) (b)

**Fig. 1:** The schematic diagram of $Si/SiO_2$ DBR stacks and field distribution.

**Table 1:** The thickness of the $Si/SiO_2$ layers at different center wavelengths.

| S.N. | Center Wavelength 'λc' (nm) | Thickness of DBR ($Si/SiO_2$)(nm) | Lattice Constant 'a'(nm) |
|---|---|---|---|
| 1 | 400 | 28 / 69 | 97 |
| 2 | 600 | 42/103 | 145 |
| 3 | 800 | 57/137 | 194 |
| 4 | 1000 | 71/172 | 243 |

In this numerical simulation includes boundary conditions such as periodic boundary conditions (PBC) in x and y-axis. This boundary condition chooses at equivalent to infinite

structures. Next, the perfect match layer (PML) in the z-axis is useful to eliminate the outward propagating energy that impinges on the boundaries.

## 3. Results and discussion

### 3.1 Photonic band gap investigation

As compared to the various conventional materials, photonic crystals are preferred due to the best light confinement among the air medium and selected materials. Furthermore, the radiation losses are zero at the sharp band edges.[20-21] Here, the photonic band gap diagram of the 1D photonic crystals can be adjusted by changing the various structural parameters, such as each layer thickness, materials selection, and center wavelength of incident light. According to the photonic crystal theory, changing the center wavelength is proportionally equal to resizing the band structure, as shown in Fig. 2. Fig. 2(a) depicts the reflectivity spectra and photonic band gap of 1D PCs ($Si/SiO_2$). The reflectivity is enhanced with respect to the number of DBR layers. With the effect of the center wavelength of 400 nm, the reflectance and photonic band gap varied from 300-570 nm, as shown in Fig. 2(a). Further, it was observed that enhancement of the number of DBR stacks increased the oscillation of electromagnetic light waves, suppressing them, which helped to generate better confinement of light within the band gap in an omnidirectional way.[22] However, we have varied the 1 DBR to 10 DBR stacks and noticed the highest (or broader) reflectance, with 99.9% starting from 5 DBR stacks. Fig. 2(b) shows the reflectance spectra of 1DBR to 5 DBR of $Si/SiO_2$ 1D PCs under the center wavelength of 600 nm. Overall, the total photonic band gap of 400 nm was obtained from and varies from 455-855 nm. The improved shifted and broader PBG was achieved by the thickness of the DBR layers. In photonic crystals, the transverse electric field guiding is accomplished by the distribution of reflected light within the 1D PCs. By employing the plane wave method, the photonic band gap was calculated and studied their properties. Saravanan and Dubey (2020) reported the photonic band gap shifting towards the longer wavelength with respect to the increased number of 1D photonic crystal (DBR) layers.[19]

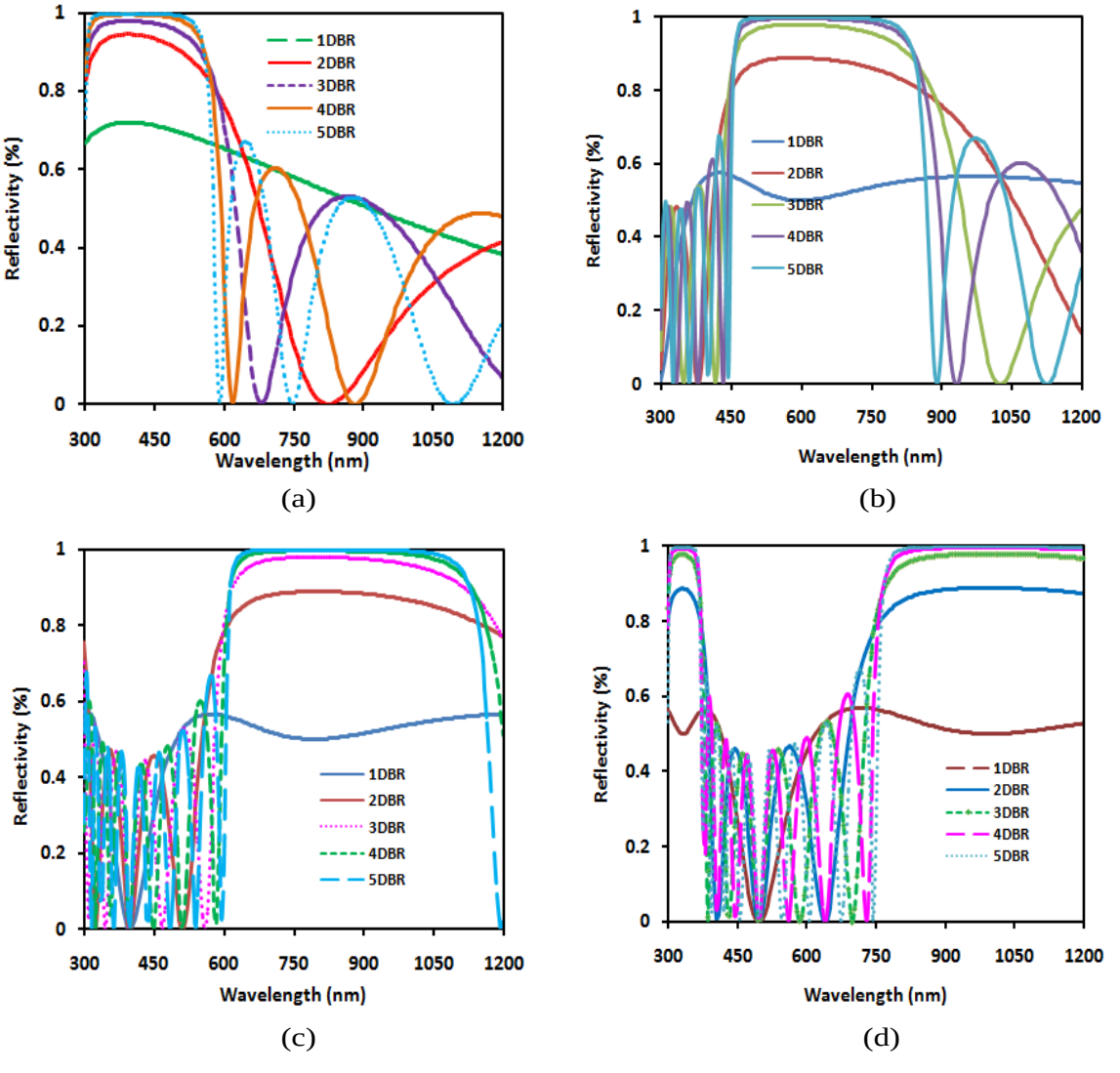


**Fig. 2:** The reflectivity of center wavelength of 1DBR-5DBR structures (a) 400 nm, (b) 600 nm, (c) 800 nm and (d) 1000 nm.

Fig. 2(c) depicts the reflectance spectra of 1D photonic crystals of Si/$SiO_2$ alternative layers under 800 nm center wavelength. Totally, we have calculated the photonic band gap of 530 nm and vary from 615-1145 nm. As compare others, the wide photonic band gap noticed under the center wavelength of 800 nm. Saravanan and Dubey experimentally reported the enhancement of a number of alternative layers ($SiO_2$/$TiO_2$) and generated the photonic band gap shifting towards the longer wavelength.[21] Furthermore, the reflectance study was enhanced with center wavelength of 1000 nm, as shown in Fig. 2(d). The 1D photonic crystals of Si/$SiO_2$ layers varied from 1DBR-10DBR and found maximum reflectivity at 5DBR layers with 99.99%. The reflectivity starts from 760 nm and continuing the bandgap. The center wavelength increasing as 400, 600, 800 and 1000 nm correspondingly the photonic band gap also increasing such as 270, 400, 530 and > 430 nm, respectively. Here, the reflectivity study was carried out from 300 to 1200 nm region. These photonic band gap calculations determined by the Bragg's condition. This reflectivity investigation was carried out under normal incidence angle (θ°) with air mass 1.5G. Furthermore, the reflectivity of 15DBR (400+600+800nm) stacks is shown in Fig. 3. The wider photonic band gap noticed from 300 to 1150 nm spectral region. With the effect of various center wavelength combinations of DBR showed highest reflectivity in the UV-Visible and infrared region.

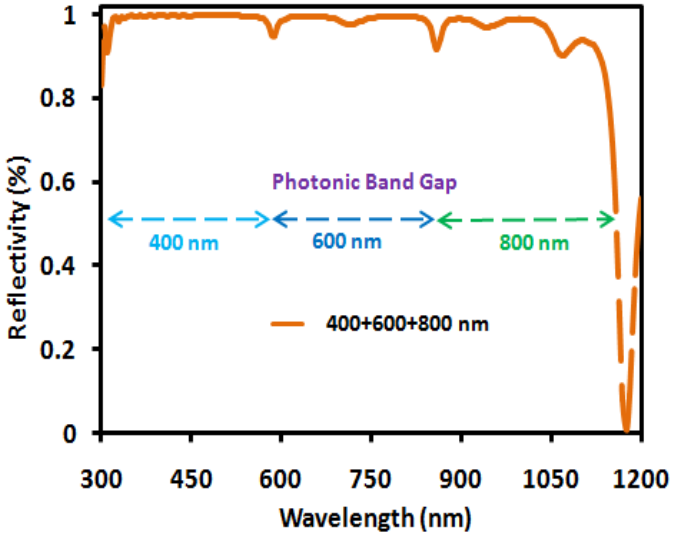


**Fig. 3:** The reflectivity of 15 DBRs (400+600+800 nm) structures.

By incrementing the incident angle, the reflectivity was shifting towards the shorter wavelength region, as reported by Gondek and Karasinski.[22] The resulting modulated structures were formed from multiple DBR layers of dielectric (Si/$SiO_2$) materials in which each layer partially reflects and transmits the optical wave. The spectral wavelength range was calculated from 300 to 1200 nm. Beyond 1200 nm, the percentage of the solar spectrum absorption is less, and high energy losses are noticed in solar cells due to unabsorbed photons, as reported by Joseph Day.[23] Saravanan and Dubey experimentally reported that higher and broader reflectivity was noticed due to the number of alternative layers.[21] The broader PBG was noticed with the effect of a higher center wavelength with ~100% reflectivity.[23] The reflected waves combine and provide constructive interference, and the layers act as a perfect mirror back reflector. This DBR layer reflectivity (R) is defined as,

$$R = \left[\frac{n_0(n_2)^{2N} - n_s(n_1)^{2N}}{n_0(n_2)^{2N} + n_s(n_1)^{2N}}\right]^2 \quad (3)$$

where '$n_0$' is the refractive index of the air (background) medium, '$n_1$' is the refractive index of the silicon, $n_2$ is the refractive index of the $SiO_2$, '$n_s$' is the substrate refractive index and 'N' is the number of stacks (or repeated pairs).[24] Moreover, when the 5DBR layers of the maximum reflectance reached up to 99.84% with a wider band gap.

### 3.2 Amorphous silicon thin film solar cells

For the enhancement of the light trapping mechanism, 5DBR with different center wavelengths was integrated as a backside reflector in a-Si solar cells, which includes ITO-anti-reflection coatings (20 nm), active (40 nm), and top-ITO nanogratings. Here, metal/dielectric nanogratings are an effective approach in solar cells for the improvement of the light trapping mechanism.[25] Among these, the center wavelength ($\lambda_c$) of 400 and 800 nm DBRs integrated solar cells generated the less optical performance (5.43% and 4.88%) in longer wavelengths. The absorption spectra for 5 DBR (distributed Bragg's reflector) with nano gratings generate the highest cell performance of 5.84 % under λc=600 nm center wavelength. The incidence light absorption records the total power of absorbed within the domain, such as periodic boundary condition (PBC, X- and Y-axis) and perfectly matched layer (PML, Z-axis). This domain reduces the unwanted light reflection and interaction and helps to collect the entire incident light by increasing reflection or lifetime. The absorption was determined by A (λ) =1-T (λ) -R (λ), here, T is the transmittance and R is the reflectance. By considering plane wave incident on the solar cell, the reflectance and transmittance calculated by RCWA method which solves the electromagnetic field problem using Maxwell equations with PBC and PML boundary conditions.[26-27]

Fig. 4 shows the schematic diagram of a thin film a-Si solar cell integrated with 5DBR (800 nm λc), ARC-ITO (108 nm), top-ITO nanogratings, a-Si active layer (40 nm) and bottom-Ag asymmetrical nanogratings. The thickness of the Ag-metallic and ITO-dielectric nano gratings is 20 nm, and the distance (D=20nm) between the gratings is maintained. With the addition of dual gratings and 5DBR stacks, the a-Si solar cell performance was carried out by using center wavelengths, like 400, 600, 800, and 1000 nm. Fig. 5 shows the absorption (%) of a-Si solar cells with the integration of ARC, active layer and DBR layers. As compared to different solar cells, 5DBR of 800 nm center wavelengths showed increased performance due to the high photonic band gap, further extending this investigation by changing the solar cell structures.

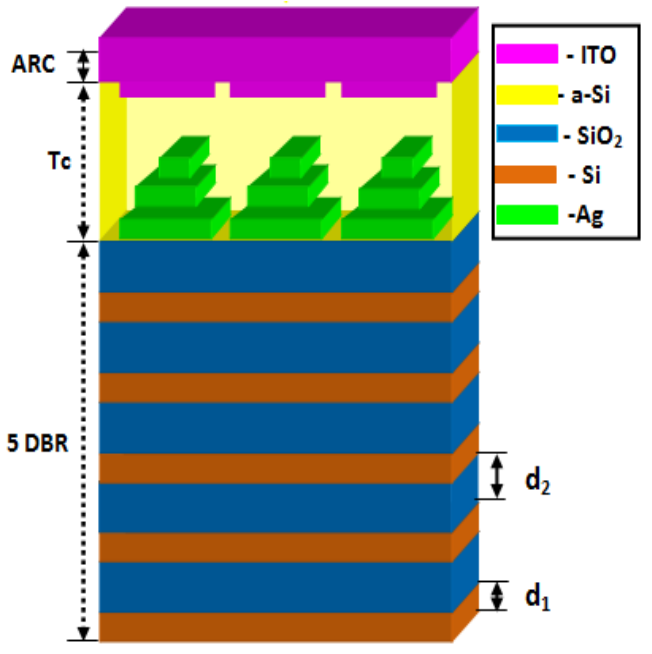


**Fig. 4:** The illustration of thin film a-Si solar cells.

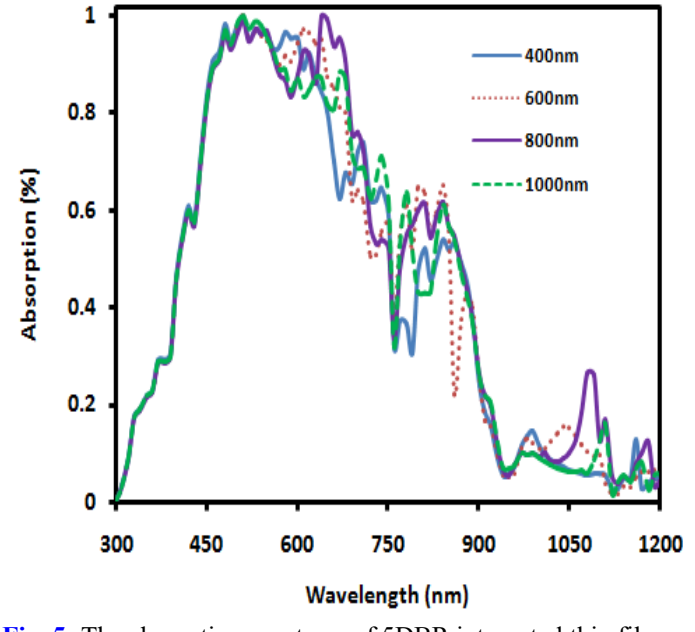


**Fig. 5:** The absorption spectrum of 5DBR integrated thin film a-Si Si solar cells with various center wavelengths.

Fig. 6 depicts the absorption spectra of the complete solar cells with different back reflectors under 800 nm center wavelengths (λc). It is seen that the absorption is enhanced with dual grating with distributed Bragg's reflector (DBR) based ultra-thin solar cells (solid line-pink). In this cell structure, the incident light, when it reaches the top-ITO grating, spreads (allows), reduces the back reflection and diffracts the photons at various angles or directions. Next, the bottom asymmetrical Ag-nanograting, also an important part to enhance in coupled light, is further diffracted and reflected back to the active layer (Yellow dotted line). Overall, the dual grating and DBR integrated structure significantly broader and stronger performance in longer wavelength regions. The periodicity in the lateral X-axis (direction), the incoming light coupled back into the active region by the reflectivity of DBR layers, which depends on the center wavelength and polarization conditions.[16] These structures enable a strong light-matter interaction due to increased photon absorption. These electric field profiles significantly enhance the guided mode between the gratings. The collection of the light photons enhanced with the 5DBR and dual gratings was integrated into solar cells, and further, the current density and electric field were calculated. The current density (Jsc) was also calculated by

$$J_{sc} = \frac{e}{hc}\int_{300}^{1200} \lambda A(\lambda)\frac{dI}{d\lambda}d\lambda \quad (4)$$

where λ-wavelength, c-the speed of light, h-plank's constant, A-the absorption in the active region, I-the incident light spectrum ($Wm^{-2}$ $nm^{-1}$).[27]

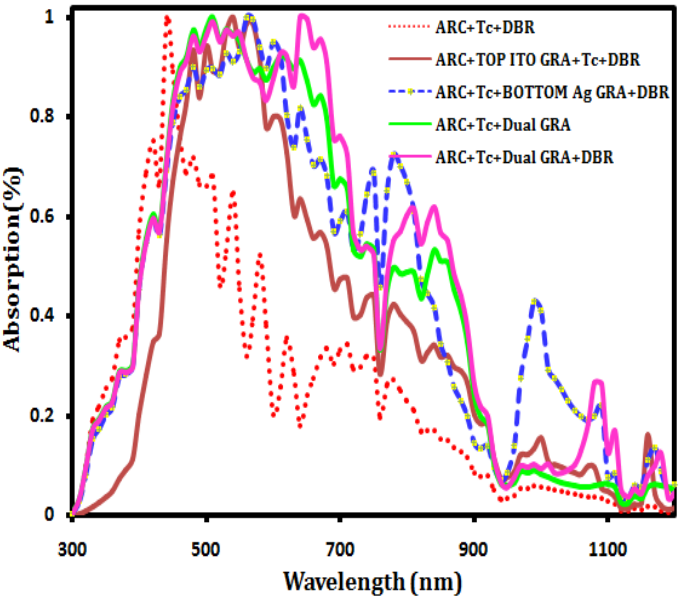


**Fig. 6:** Absorption spectra of amorphous silicon thin film solar cells with different structures.

Fig. 7 (a) shows the electric field distribution at 639 nm wavelengths, the diffraction pattern noticed in the active region, and bottom metallic-Ag asymmetric structures. Further, top-ITO gratings are helping to spread the incident light into the active region. Here, the filed distribution and intensity decrease at the lower DBR stacks. The red and cyan color shows the strong field intensity within the solar cells. Fig. 7(b) depicts the strong electric field at the end of the top-ITO gratings, and the wave-like nature that appeared in the DBR layers (λ=700 nm). In DBR, the partial light reflects back into the active region and remains transmitted towards the lower region. The surface-guided mode is shown in the active region and is depicted in cyan color. However, a very low intensity of light was observed in the DBR layers. Fig. 7(c) depicts the surface-guided modes, Fabry-Perot resonance modes, and low

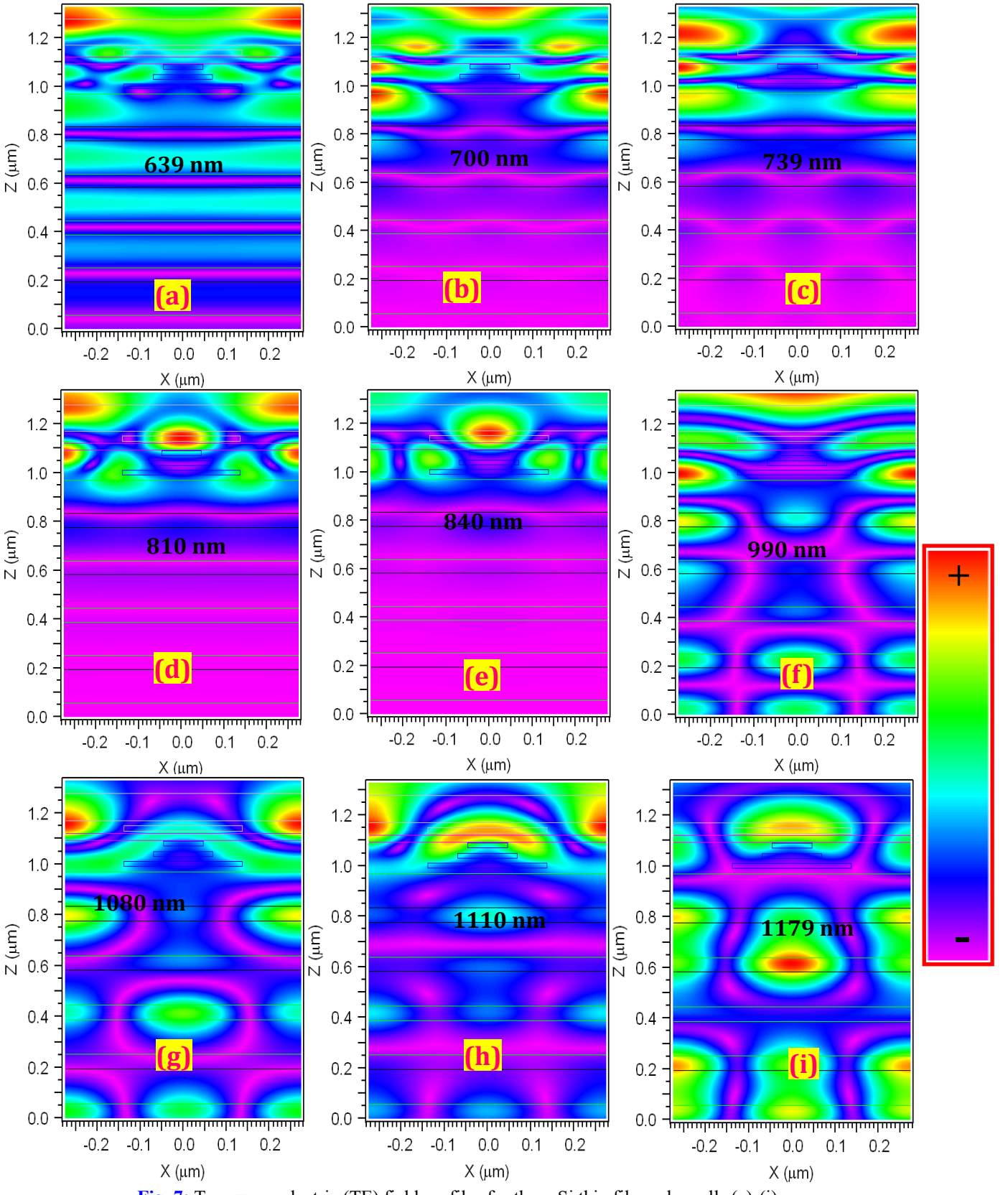


**Fig. 7:** Transverse electric (TE) field profiles for the a-Si thin film solar cells (a)-(i).

field intensity observed at 739 nm. The wave-like nature increased in the DBR layers. The back reflector (metal/dielectric) prevents the light from escaping from the back side and reflecting back completely. Figs. 7(d)-(e) showsthe strong field in the ARC region and metallic gratings. The light interaction reduced at 810 and 840 nm incident spectral region. In the near-infrared spectral region, sharp absorption peaks were noticed, which reduced the collection of photons. Similarly, the field intensity reduced considerably at 990, 1080, 1110, and 1179 nm, as shown in Figs. 7(f)-(i) due

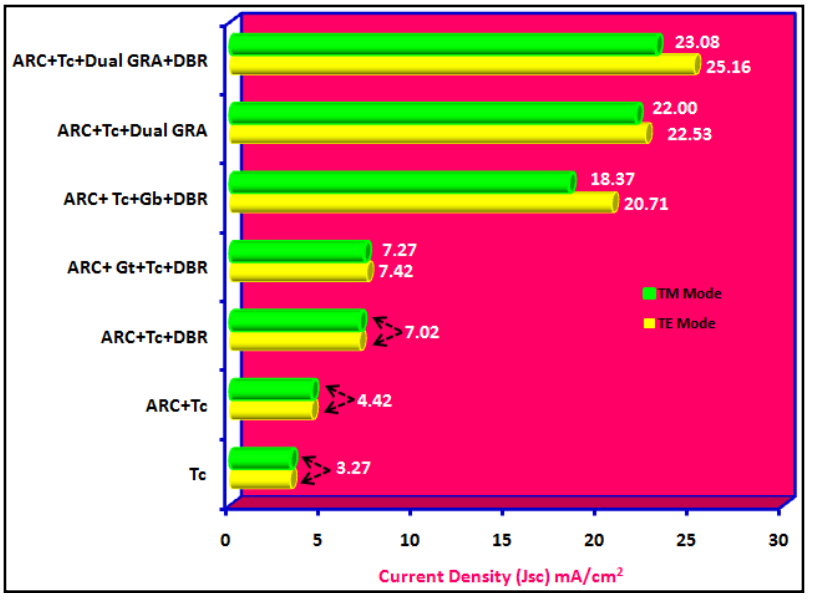


**Fig. 8:** The Jsc of different a-Si Si solar cells.

to the unabsorbed light photons which are to be focused. However, guided modes are enhanced in the longer wavelengths such as 1080, 1110, and 1179 nm.[30] The distinct structures are enabling a strong light-matter interaction due to that increased the photon absorption. Through these electric field profiles shows significantly enhance the guided mode between the gratings. However, the induced TE field is showing Fig. 7. To observe the best electric field distribution within the active region, we have simulated and optimized 1DPC as omnidirectional reflector used as a backside reflector in a-Si Si solar cells. Overall, these results show dual grating structure induces the electron-hole recombination effect and brings a better light absorption in longer wavelength (Fig. 4). The optimal performance of various designed solar cell structures are compared in Table 2 as reported by various researchers.

Fig. 8 explains the current density with respect to the various amorphous silicon solar cells. Without the nanogratings and DBR layers, the reference cell (Tc) reached up to 3.27 mA/cm$^2$ of current density. Also, with the integration of the ARC layer (ARC+Tc) and DBR (ARC+Tc+DBR), cell structures achieved 4.42 and 7.02 mA/cm$^2$. Next, the top grating (ARC+Gt+Tc+DBR) and bottom grating (ARC+Tc+Gb+DBR) integrated cell structure increased the light-harvesting due to the scattering and reflection of incident photons.

These cell structures obtained enhanced current densities of 7.27 (TM mode) and 7.42 mA/cm$^2$ (TE mode) for ARC+Gt+Tc+DBR and 18.37 (TM) and 20.71 mA/cm$^2$(TE) for ARC+Tc+Gb+DBR structure. Furthermore, dual gratings integrated without (ARC+Tc+Dual GRA) and with DBR layer (ARC+Tc+Dual GRA+DBR) showed the highest current density of 22 and 22.53 mA/cm$^2$ (TE) and 23.08 (TE) and 25.16 (TM). The thin film solar cell performance can be enhanced by using plasmonic effects or modes, as reported by various researchers. The surface-guided modes, localized fields, and surface excitations are the few plasmonic effects that help to enhance the light trapping mechanism. However, the proposed work majorly focused on photonic effects due to their significant role in light harvesting mechanisms. The optimal values of structural and optical parameters are responsible for better light confinement in the a-Si active region. These 1D photonic crystals are totally reflected and act as a perfect reflector in the a-Si Si solar cells. In the proposed work, experimentally fabricate with the same parameters (Section 2). For that, sol-gel spin-coater (or dip coater), electrochemical etching, chemical vapor deposition (CVD), plasma-enhanced chemical vapor deposition (PECVD), lithography, and sputtering techniques can be used. A simple sol-gel spin coater is an easy method for fabricating Si/$SiO_2$

**Table 2:** The comparison of various solar cell performances with the reduced active region.

| Active | Thickness | No. of DBR Layers | η (%) | Jsc (mA/cm$^2$) | Ref. |
|---|---|---|---|---|---|
| c-Si | 50 nm | DBR ($SiO_2$/a-Si) | 14.93 | 22.71 | [1] |
| c-Si | 10 µm | DBR ($Si_3N_4$/Si) | 13.2 | 27.5 | [28] |
| c-Si | 2 µm | DBR (c-Si/$SiO_2$) | 31.3 | - | [29] |
| c-Si | 41 nm | DBR (Si/$SiO_2$) | 16.8 | 19.69 | [6] |
| c-Si | 1 µm | DBR (Si/$SiO_2$) | 20.95 | 24.51 | [12] |
| Si | 40 nm | DBR (a-Si/$SiO_2$) | 14.93 | 22.71 | [30] |
| a-Si | 40 nm | DBR (Si/$SiO_2$) | - | 25.16 | Present work |

DBR layers. These structures can adhere to the required substrate, and the substrate can be grooved by electrochemical etching or mechanical force to integrate nanogratings. Next, Ag nanogratings can be deposited on active layer by sputtering. Finally, ARC can be coated by sol-gel spin coater of CVD technique.

## 4. Conclusion

In this paper, we focused on the influence of optimized DBR layers by changing the center wavelengths (λ=400, 600, 800, 1000 nm). With the assistance of better DBR layers, Ag triangular nanogratings and ITO-ARC were integrated in thin film a-Si solar cells. Using RCWA method, DBR and Ag nanogratings showed an extremely low-loss and serve as a backbone of the solar cell device by enhancement of light harvesting due to unusual way of light reflectivity and scattering mechanism. By influence of optimized 5DBR stacks and Ag nanogratings achieved the maximum current density ~25.16 mA/cm$^2$ within 40 nm thick active by preventing the recombination losses of electron and hole pairs. Finally, the 1D photonic crystals ($Si/SiO_2$) and diffractive ITO/Ag nanogratings combination is capable to improve light harvesting mechanism in thin film solar cells. At nanoscale level engineering, this design could be fulfilling the future energy needs by fabrication of a-Si thin film solar cell with advanced technology (PVD, CVD). It leads a new generation of photonics based amorphous silicon solar cells with low-cost and flexible device.

## Acknowledgement

We authors would like to thank Principal and Management of Swarnandhra College of Engineering & Technology (Autonomous), Narsapur (AP), India for providing research facilities.

## Conflict of Interest

There is no conflict of interest.

## Supporting Information

Not applicable.

## References

[1] Rebecca Saive, Light trapping in thin silicon solar cells: A review fundamentals and technologies, *Progress in Photovoltaics: Research and Applications*, 2021, **29**, 1125-1137, doi: 10.1002/pip.3440

[2] H. L. Chen, A. Cattoni, R. D. Lepinau, A. W. Walker, O. Höhn, D. Lackner, G. Siefer, M. Faustini, N. Vandamme, J. Goffard, B. Behaghel, A 19.9%-efficient ultrathin solar cell based on a 205-nm-thick GaAs absorber and a silver nanostructured back mirror, *Nature Energy*, 2019, **4**, 761-767, doi: 10.1038/s41560-019-0434-y.

[3] Z. Durmaz, S. Husein, R. Saive Thin silicon interference solar cells for targetted or broadband wavelength absorption enhancement, *Optics Express*, 2021, **29**, 4324-4337, doi: 10.1364/OE.413294.

[4] F. X. Abomo Abega, A.Teyou Ngoupo, J. M. B. Ndjaka, Numerical design of ultrathin hydrogenated amorphous silicon - based solar cell, *International Journal of Photoenergy*, 2021, **2021**, 7506837, doi: 10.1155/2021/7506837.

[5] Y. Fink, J. N. Winn, S. Fan, C. Chen, J. Michel, J. D. Joannopoulos, E. L. Thomas, A dielectric omnidirectional reflector, *Science*, 1998, **282**, 1679-1682, doi: 10.1126/science.282.5394.1679

[6] M. R. Venumbaka, N. Akkala, S. Duraisamy, S. Sigamani, P. K. Poola, B. C. Marepally, Performance of $TiO_2$, Cu-$TiO_2$, and N-$TiO_2$ nanoparticles sensitization with natural dyes for dye sensitized solar cells, *Materials Today: Proceedings*, 2022, **49**, 2747-2751, doi: 10.1016/j.matpr.2021.09.281.

[7] S. Saravanan, Optical Pathlength Enhancement in Ultrathin Silicon Solar Cell Using Decorated Silver Nanoparticles on Aluminium Grating, *Nanosystems: Physics, Chemistry, Mathematics (NPCM)*, 2020, **11**, 86-91, doi: 10.17586/2220-8054-2020-11-1-86-91.

[8] R.S. Dubey and S. Saravanan, Light trapping enhancement in thin film silicon solar cells with different back reflector, *International Journal of Electrical Components and Energy Conversion (IJECEC)*, 2017, **3**, 83-87, doi: 10.11648/j.ijecec.20170305.11.

[9] J. Du, Y. An, C. Zhang, C. Zhu, X. Li, D. Ma, Photonic design and electrical evaluation of dual-functional solar cells for energy conversion and display applications, *Nanoscale Research Letters*, 2019, **14**, 1-9, doi: 10.1186/s11671-019-2901-6.

[10] R. S. Dubey, S. Saravanan, S. Kalainathan, Performance Evaluation of Thin Film Silicon Solar Cell Based on Dual Diffraction Grating, *Nanoscale Research Letters*, 2014, **8**, 688-693, doi: 10.1186/1556-276X-9-688.

[11] Rahul Dewan, Dietmar Knipp, Light trapping in thin film silicon solar cells with integrated diffraction grating, *Journal of Applied Physics*, 2009, **106**, 074901-1-7, doi: 10.1063/1.3232236

[12] Anna Starczewska, and Miroslawa Kepinska, Photonic crystal structures for photovoltaic applications, *Materials*, 2024, **17**, 1196, doi: 10.3390/ma17051196.

[13] S. Karthika, R. Manoharan, S. Saif, T. Priya Rose, An optimum design of one-dimensional photonic crystal for solar cell applications, *IOP Conf. Series: Materials Science and Engineering,* 2022, **1219**, 012047, doi: 10.1088/1757-899X/1219/1/012047.

[14] Rahul Kumar Ganawar, A.K. Pathak, and Santhosh Kumar, Recent progress in photonic crystal devices and their applications: A review, *Photonics*, 2023, **10**, 1199, doi: 10.3390/photonics10111199.

[15] Andrea Cordaro, R. Muller, S.W. Tabernig, N. Tucher, P. Schygulla, O. Hihn, B, Blasi, and A. Ploman, Nanopatterned back-reflector with engineered near-field/far-field light scattering for enhanced light trapping in silicon –based multijunction solar cells, *ACS Photonics*, 2023, **10**, 4061-4070, doi: 10.1021/acsphotonics.3c01124.

[16] S. Sigamani, R.S. Dubey, S. Kalainathan, Optimization of distributed Bragg's reflectors in thin film solar cells, *Materials Today: Proceedings*, 2023, **89**, 8-13, doi: 10.1016/j.matpr.2023.05.540.
[17] N. Feng, J. Michel, L. Zeng, J. Liu, C. Hong, L. C. Kimerling, Design of highly efficient light-trapping structures for thin-film crystalline silicon solar cells, *IEEE Transactions on Electron Devices*, 2007, **54,** 1926-1933. doi: 10.1109/TED.2007.900976.
[18] D. Zhang, W. Hu, Y. Zhang, Z. Li, B. Cheng, G. Yang, Experimental verification of light localization for disordered multilayers in the visible-infrared spectrum, *Physical Review B*, 1984, **50**, 9810, doi: 10.1103/PhysRevB.50.9810.
[19] S. Saravanan, R. S. Dubey, One-dimensional photonic crystals ($Si/SiO_2$) for ultrathin film crystalline silicon solar cells, *Nanosystems: Physics, Chemistry, Mathematics*, 2020, **11**, 189-194, doi: 10.17586/2220-8054-2020-11-2-189-194.
[20] V. A. Tolmachev, T. S. Perova, Design of one-dimensional composite photonic crystals with an extended photonic band gap, *Journal of Applied Physics*, 2006, **99**, 033507, doi: 10.1063/1.2165401.
[21] S. Saravanan, R.S. Dubey, Ultraviolet and visible reflective $TiO_2/SiO_2$ thin films on silicon using sol-gel spin coater, *Nanosystems: Physics, Chemistry, Mathematics*, 2021, **12**, 311-316, doi: 10.17586/2220-8054-2021-12-3-311-316.
[22] E. Gondek, P. Karasinski, 1-D Photonic crystals for Photovoltaics, *Photonics Letters of Poland*, 2012, **4**, 75-77, doi: 10.3390/ma17051196.
[23] J. Day, S. Senthilarasu, T. K. Mallick Improving spectral modification for applications in solar cells: A review, *Renewable Energy*, 2019, **132**, 186-205, doi: 10.1016/j.renene.2018.07.101.
[24] C.J.R. Sheppard, Approximate calculation of the reflection coefficient from a stratified medium, *Pure and Applied Optics: Journal of the European Optical Society Part A*, 1995, **4**, 665, doi: 10.1088/0963-9659/4/5/018.
[25] F. Qin, H. Zhang, C. Wang, J. Zhang, C. Guo, Anodic aluminum oxide nanograting for back light trapping in thin c-si solar cells, *Optics Communications*, 2014, **331**, 325-329, doi: 10.1016/j.optcom.2014.06.049.
[26] L. Zhao, Y. H. Zuo, C. L. Zhou, H. L. Li, H.W. Diao, W. J. Wang, A highly efficient light-trapping structure for thin-film silicon solar cells, *Solar Energy*, 2010, **84**, 110-115, doi: 10.1016/j.solener.2009.10.014.
[27] S. Saravanan, R. S. Dubey, and S. Kalainathan, Design and analysis of thin film silicon solar cells using FDTD method, *Procedia Materials Science*, 2015, **10**, 301-306, doi: 10.1016/j.mspro.2015.06.054.
[28] R. S. Dubey, K. Jhansirani, S. Singh, Investigation of solar cell performance using multilayer thin film structure ($SiO_2/Si_3N_4$) and grating, *Results in Physics*, 2017, **7**, 77-81, doi: 10.1016/j.rinp.2016.11.065.
[29] P. Bermel, C. Luo, L. Zeng, L. C. Kimerling, J. D. Joannopoulos, Improving thin-film crystalline silicon solar cell efficiencies with photonic crystals, *Optics Express*, 2007, **15**, 16986-17000, doi: 10.1364/OE.15.016986.
[30] S. Saravanan, R. S. Dubey, S. Kalainathan, M. A. More, D. K. Gautam, Design and optimization of ultrathin crystalline silicon solar cells using an efficient back reflector, *AIP Advances*, 2015, **5**, 057160, doi: 10.1063/1.4921944.